EXPLOITING SHAPED COMBS WITHIN FM ACCELEROMETERS FOR LOW-NOISE AND WIDE DYNAMIC RANGE APPLICATIONS

Christian Padovani[1], Luca Pileri[1], Gabriele Gattere[2] and Giacomo Langfelder[1]
[1]Politecnico di Milano, ITALY and
[2]STMicroelectronics, ITALY

2025 IEEE 38th International Conference on Micro Electro Mechanical Systems (MEMS) | 979-8-3315-0889-0/25/$31.00 ©2025 IEEE | DOI: 10.1109/MEMS61431.2025.10918239

ABSTRACT

The work presents the first frequency-modulated (FM) in-plane accelerometer exploiting shaped combs as frequency-tuning mechanism. Their inherent advantage lies in that, while the overall tuning coefficient is unaltered with respect to former implementations based on parallel-plate tuning, the resonant-mode motion amplitude can be increased, without limitations from parallel-plate gaps. This enables lowering equivalent frequency noise down to ~15 μg/√Hz while guaranteeing a full-scale range at about 60 g, within 1.8-mm² overall area. Such performances are demanded by all applications simultaneously requiring low noise and large dynamic range.

KEYWORDS

MEMS, accelerometer, frequency-modulated, shaped combs, comb fingers, frequency tuning

INTRODUCTION

Capacitive transduction in MEMS usually splits between area variation (combs) for highly linear large displacements, and gap variation (parallel plates) for large transduction within small displacements. Among other topologies, shaped comb fingers (SCF) were studied to provide generic (both area and gap variation) force-displacement laws [1]: however, the use of such arbitrary shapes was so far limited [2], due to constraints associated to the positioning of design (layout) points within the final mask grid (resolution usually >10 nm). In turn, the shaped-comb size needed to be large, to minimize differences with respect to the nominal profiles.

Within this context, several MEMS exploit the intrinsic nonlinearity of parallel-plate capacitors (so-called electrostatic softening) for sensing applications. It is the case of some FM accelerometers, where the proof mass displacement under accelerations induces a change in electrostatic stiffness, thus in resonance [3, 4]. This work combines the two concepts by embedding, within an accelerometer, the shaped combs for tuning purposes. The benefit over parallel-plate (PP) solutions [4] is the chance to increase the resonant motion by about 10 times, thus reducing frequency noise by the same amount, avoiding pull-in related issues. The used process, besides, enables keeping a shaped-comb cell in the grid, within 11 μm only.

SHAPED COMB APPLICATION

The most straightforward application is the one regarding the continuous mode-reversal FM accelerometer, which exploits the nonlinearity of the electrostatic force of parallel plates to induce a frequency modulation with continuous time reversal. The accelerometer works according to the following scheme [5]: an antiphase, tuning-fork, mode (*f*-mode) is kept in resonant oscillation

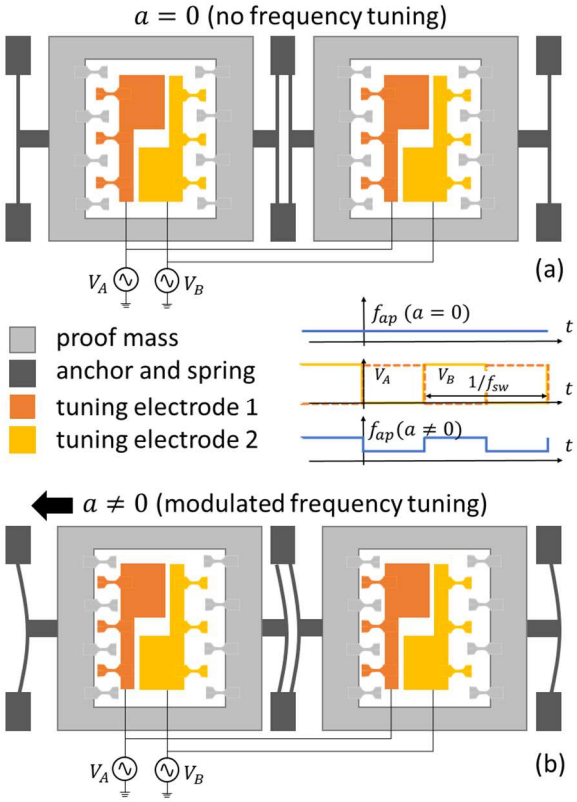

Fig. 1: the sensor relies on a pair of masses linked by a tuning fork, with shaped-comb tuning electrodes nested inside (shown as yellow and orange stators). Without accelerations (a), their periodic bias at f_{sw} yields no antiphase resonance modulation. In presence of accelerations (b), resonant frequency modulation (FM) at f_{sw} arises, proportional to the inertial force intensity.

via conventional combs. Nested within the two half masses are tuning electrodes biased with alternate tuning waves (Fig. 1a). Under accelerations acting on the in-phase mode (a-mode, Fig. 1b), they provide a modulation of the stiffness, thus of the frequency. By demodulating the digitized frequency value, the acceleration is retrieved. The in-phase mode is sized above 4 kHz, to provide wide full-scale and good vibration immunity, while the antiphase mode is positioned around 25 kHz, above the audio range.

The expression of the electrostatic force acting on a mass, for a generic shape of fingers moving along the x axis and with variable gap as a function of x is:

$$F_{tun} = \frac{\Delta V^2}{2}\frac{d}{dx}\int_0^l \frac{\epsilon_0 h N}{g(x)}dx \qquad (1)$$

where h is the height of the process and l, g, N are the facing length of the electrodes, their gap towards the mass, and the number of their cells, respectively. By exploiting a Taylor expansion, all the coefficients with respect to the displacement can be retrieved. For small displacements relative to the facing length and for suitable geometries, the

expansion can be stopped at the second order as in Eq. (2):

$$F_{tun} = (Q_t x^2 + L_t x + C_t)\Delta V^2(t) \quad (2)$$

where Q_t, L_t and C_t are respectively the quadratic, the linear and the constant term. In case of a conventional parallel-plate solution, the terms would be the following:

$$C_t = \frac{\epsilon_0 h l N}{2g^2}$$
$$L_t = \frac{2}{g} \cdot C_t \quad (3)$$
$$Q_t = \frac{3}{g^2} \cdot C_t$$

The electrostatic frequency modulation is retrieved by placing, nested in the masses, pairs of SCF tuning stators (#A, #B) and applying antiphase sinusoidal voltages, leading to the following voltage difference with the rotor:

$$\Delta V_A = V_{rot} - V_A = V_{DC} - V_{sin}\sin(\omega_{sw} t)$$
$$\Delta V_B = V_{rot} - V_B = V_{DC} + V_{sin}\sin(\omega_{sw} t) \quad (4)$$

where V_{rot} is the rotor voltage, V_{DC} is the static differential voltage between the SCF and the rotor and V_{sin} is the amplitude of the sinewave at ω_{sw}. The anti-phase term of the electrostatic force, now naming x_{ph} and x_{ap} the in-phase and anti-phase motion, respectively, is written as:

$$F_{tun,AP} = [-8Q_t x_{ph} V_{DC} V_{sin}\, sin(\omega_{sw} t) + 2L_t V_{DC}^2 + 2L_t V_{sin}^2\, sin^2(\omega_{sw} t)]\, x_{ap} \quad (5)$$

leading to an anti-phase frequency variation with respect to the rest value $f_{0,ap}$:

$$f_{ap} = f_{0,ap}\{1 - k_{ap}^{-1}[4Q_t V_{DC} V_{sin} x_{ph}\, sin(\omega_{sw} t) + L_t V_{DC}^2 + L_t V_{sin}^2\, sin^2(\omega_{sw} t)]\} \quad (6)$$

In the expression above one can find a static downshift of the resonant frequency, a sinusoidal modulation and a spurious tone at twice the modulating frequency, which will be notched out. Since the information about the in-phase displacement lies at ω_{sw}, the signal needs to be demodulated around this frequency, leading to the following overall scale-factor of the accelerometer:

$$SF = \frac{\Delta f_{ap}}{\Delta a} = \frac{V_{DC} V_{sin} Q_t}{\pi^2 k_{ph}} \frac{1}{f_{0,ap}} \quad (7)$$

Considering the standard implementation of a time-switched accelerometer exploiting PP as tuning electrodes, and by substituting the Q_t expression of Eq. (3) in Eq. (7), the SF can be written as reported in [6]. The new design, exploiting shaped comb fingers as tuning electrodes, aims at quantitatively holding a similar Q_t term, while avoiding the additional strong nonlinearities before and beyond the 2nd order, which drastically limit the travel range of the proof masses. The consequent increase of the antiphase motion leads to improvements of phase noise and in turn in the frequency resolution of the system [7].

The replacement of parallel plates as tuning elements, so to reach higher travel range, shall also be guided by the need to avoid a scale factor reduction. As SCFs have a lower Q_t coefficient per unit area, the sensor footprint is increased. In practice: the quadratic term of the parallel plates becomes the target value for the SCF-based tuning electrodes.

SHAPE OPTIMIZATION

The electrostatic force generated on the mass by the shaped comb fingers depends on the edge profile of the facing sides. Instead of using a rectangular one whose induced force is independent from the overlap, the shape can be defined to provide an electrostatic force with a nonlinear dependence on the relative displacement. Calling $f_1(x)$ and $f_2(x)$ the mathematical expressions of each side profile of the comb fingers along the moving direction, the total capacitance between the two surfaces, sliding each other, can be calculated as the sum of the infinitesimal capacitive contributions, which can be considered as the parallel plate ones, along the overlap length:

$$C(x) = \epsilon_0 h \int_0^x \frac{dx}{g(x)} \quad (8)$$

where $g(x) = f_1(x) - f_2(x)$ and x is the variable overlap length.

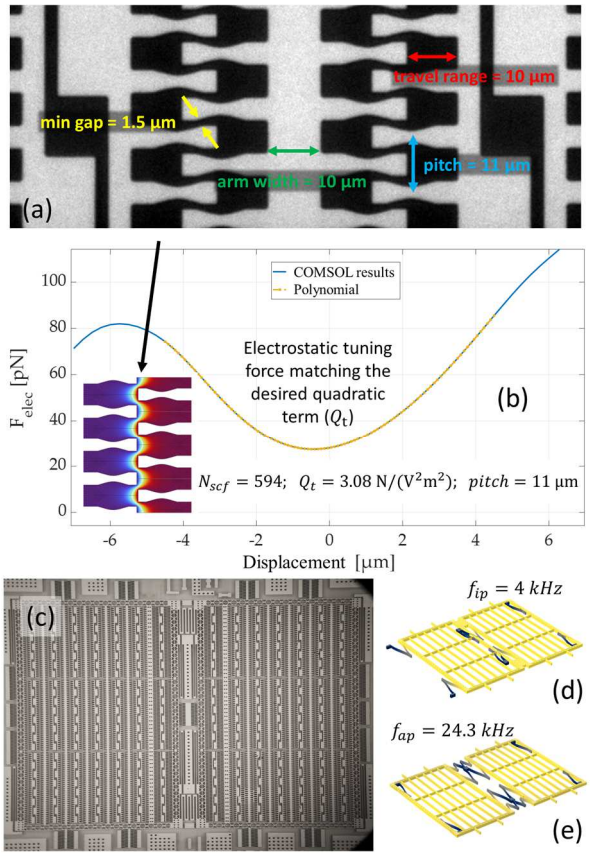

Fig. 2: SEM of the fabricated shaped comb fingers highlighting the most important dimensions (a). The reached profile of electrostatic tuning force vs displacement, simulated with COMSOL to reach the desired quadratic term and indeed the target SF, is shown in (b). A picture of the overall resulting device is reported in (c), with its in-phase and anti-phase eigenmodes and resonant frequency reported in (d-e).

As in [1], the resulting electrostatic force can be written as:

$$F_{tun} = \frac{\epsilon_0 h \Delta V^2}{2g(x)} \tag{9}$$

The suited profile for this implementation is chosen according to four main considerations and it is shown in the scanning electron microscope image of Fig. 2:

- to reach the same SF of the PP-based implementation (about 1 Hz/g), the Q_t value for a single cell needs to be evaluated. Afterwards, the number of shaped comb fingers is retrieved by equating the quadratic terms between parallel plates and shaped comb fingers:

$$Q_{t,SCF} = Q_{t,PP} \tag{10}$$

  By considering the number of PP involved in each tuning port, this leads to:

$$N_{SCF} = \frac{3}{4}\frac{\epsilon_0 h l}{g^4 Q_{t,PP}} \tag{11}$$

  The selected shape should increase the quadratic term and therefore minimize the number of needed elements. Note that the comparison is fair as it considers the same applied rotor and tuning voltages for the two implementations;
- the shape should maximize mostly the quadratic term, as all other terms represent nonlinear effects and concentration of energy at undesired tones, other than ω_{sw};
- the shape should allow a much larger anti-phase displacement of the masses with respect to the parallel plate condition, to effectively minimize the oscillator phase noise;
- finally, the in-phase resonant frequency can be slightly trimmed to further enhance the SF or, as an alternative, to decrease the number of needed SCFs.

The electrostatic behavior is validated through a 2D COMSOL model, where the comb finger profile is mathematically built and the capacitance between two facing SCFs is evaluated by applying the proper boundary condition. The stationary simulation is performed with progressive values of overlapping length, so that it is possible to retrieve the capacitance dependence on the displacement. To bypass grid-related issues, the combs shape is optimized directly within the final Cadence masks environment, so that only feasible geometries are simulated. The optimized cell is shown in Fig. 2a: its minimum gap is 1.5 µm and well matches the simulated geometries. The results of Fig. 2b show the electrostatic nonlinearity behaviour when using 594 shaped cells. Combined with the in-phase resonance reduction with respect to the previous implementation [6], they are enough to match the target SF, yielding the final design of Fig. 2c. The simulated modal shapes for the in-phase and the anti-phase motion are shown in Fig. 2d-e.

EXPERIMENTAL RESULTS

The MEMS is coupled to an analog oscillator, with FPGA-based frequency digitization and digital sinusoidal demodulation (Fig. 3). The system is then mounted on a rate table. First, slow rotations, normal to gravity, enable to accurately extract the scale factor which, at 1 Hz/g (Fig. 4a), matches simulation predictions within 20% (reasons for this deviation may lie in fringe electric fields). To cope with this deviation, the rotor bias has been increased from 15 V to 18 V. Tab. 1 reports the resonance frequency, Q-factor and scale-factor values on 5 different samples, highlighting the good part-to-part repeatability:

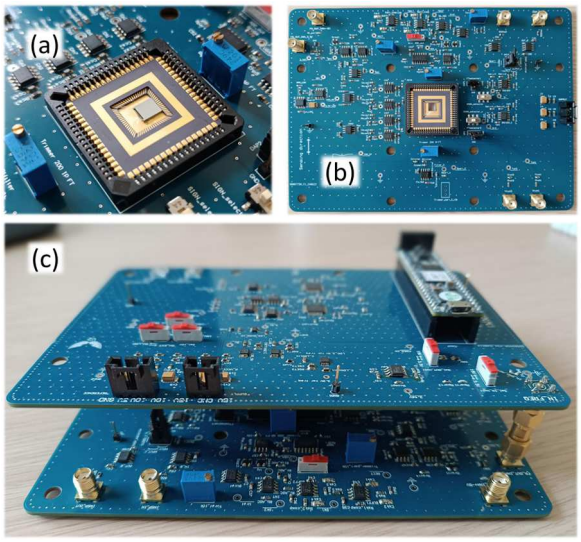

Fig. 3: the MEMS wire-bonded to the ceramic carrier (a), inserted into the analog oscillator board (b), stacked to the digital board, exploiting an FPGA module for the filtering stages and demodulation(c).

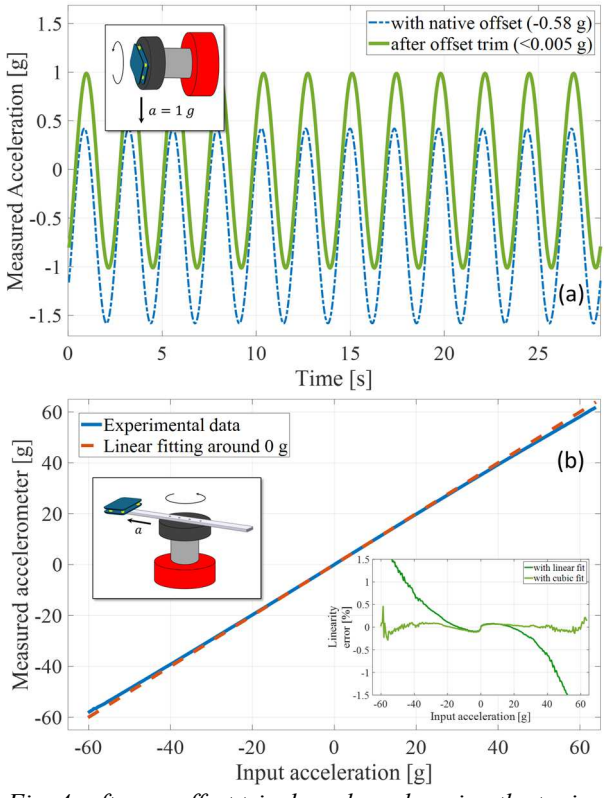

Fig. 4: after an offset trim based on changing the tuning waves DC value, the scale-factor is extracted as shown in (a). Data under 65 g are then acquired, yielding sub-0.02% linearity error after cubic compensation (b).

Table 1: Measured SF and resonances for 5 devices: to match the simulated SF, the rotor voltage has been increased from 15 V to 18 V.

Parameter	#1	#2	#3	#4	#5
f_{ph} [kHz]	4	3.99	4	3.97	4.04
f_{ap} [kHz]	24.25	24.28	24.31	24.24	24.32
SF [Hz/g]	**0.91**	**0.88**	**0.87**	**0.87**	**0.86**

Table 2: Simulated SF and resonances with ± 0.2 μm of overetch (OE).

Parameter	− OE	Nominal	+ OE
f_{ph} [kHz]	4.7	4	3.3
f_{ap} [kHz]	26	24.3	22.5
SF [Hz/g]	0.9	0.88	0.87

the small residual variability is compatible with simulation results at the process corners (see Tab. 2). Such a small variability for uncompensated devices is ascribed to a self-compensation between the quadratic term and the in-phase and anti-phase resonant frequencies in the scale-factor expression [6]. As a matter of fact, an over-etch condition induces an increase of the gap, so a reduction of Q_t and of the two resonant frequencies. Repeatability is an essential feature that must be considered while designing SCFs.

Then, with an elongation arm, centripetal accelerations of about 60-g, positive and negative, were applied to the sensor (Fig. 4b). The linearity error, extracted after the predicted cubic compensation, demonstrates sub-0.2% residuals (higher accelerations could not be provided due to setup limits). Finally, Fig. 5a shows the input-referred measured frequency noise density, confirming 16 µg/√Hz, corresponding, on a 20-Hz bandwidth, to a 130-dB dynamic range. The Allan deviation (although by now affected by extra noise coming from the DACs exploited to generate the 10-V-amplitude sinusoidal voltages) shows 10-µg stability at rather long observation intervals (Fig 5b).

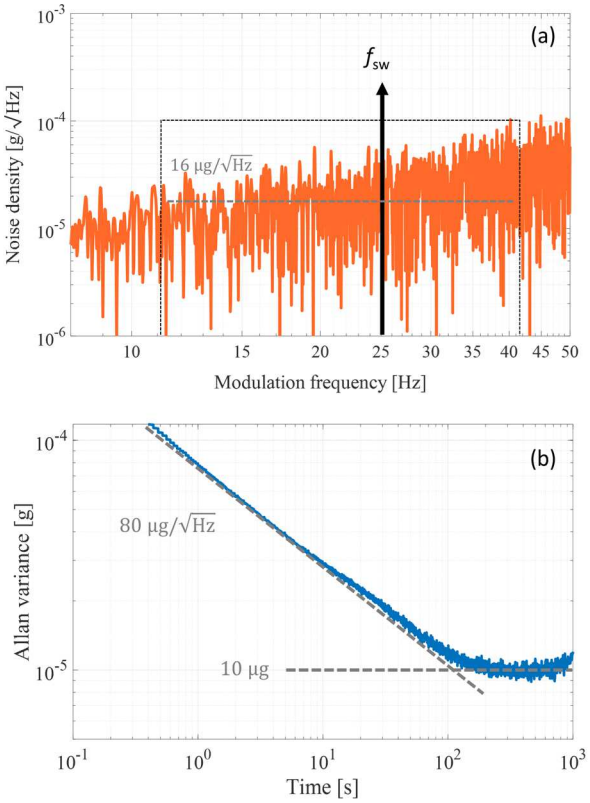

Fig. 5: measured frequency noise yields 16 $\mu g/\sqrt{Hz}$ (a). The Allan deviation (b), although by now affected by extra tuning noise, reaches 10 µg stability at 100 s.

CONCLUSION

The work presents the first time-switched frequency modulated in-plane accelerometer exploiting shaped comb fingers as tuning electrodes to provide the nonlinearity needed by the working principle and, at the same time, enabling an increase of the anti-phase displacement to improve the resolution of the system. The measurements confirm the effectiveness of the working principle and the improvement of the resolution with respect to the PP topology. As well, the robustness and the part-to-part repeatability are in line with the simulations.

REFERENCES

[1] B. D. Jensen, S. Mutlu, S. Miller, K. Kurabayashi and J. J. Allen, "Shaped comb fingers for tailored electromechanical restoring force," in *Journal of Microelectromechanical Systems*, vol. 12, no. 3, pp. 373-383, June 2003.

[2] P. Taheri-Tehrani *et al.*, "Epitaxially-encapsulated quad mass resonator with shaped comb fingers for frequency tuning," *2017 IEEE 30th International Conference on Micro Electro Mechanical Systems (MEMS)*, Las Vegas, NV, USA, 2017, pp. 1111-1114.

[3] C. Comi *et al.*, "Sensitivity and temperature behavior of a novel z-axis differential resonant micro accelerometer," *Journal of Micromechanics and Microengineering*. 26, 035006, 2016, pp. 1-11.

[4] S. A. Zotov, B. R. Simon, A. A. Trusov and A. M. Shkel, "High Quality Factor Resonant MEMS Accelerometer With Continuous Thermal Compensation," in *IEEE Sensors Journal*, vol. 15, no. 9, pp. 5045-5052, Sept. 2015.

[5] C. R. Marra, F. M. Ferrari, S. Karman, A. Tocchio, F. Rizzini and G. Langfelder, "Single-resonator, time-switched FM MEMS accelerometer with theoretical offset drift complete cancellation," *2018 IEEE Micro Electro Mechanical Systems (MEMS)*, Belfast, UK, 2018, pp. 117-120.

[6] C. Padovani, R. Nastri, L. Gaffuri Pagani, P. Frigerio, F. Rizzini and G. Langfelder, "Continuous Mode-Reversal FM Accelerometer With 60-g FSR, 10-µg/K Drift, and VRE Rejection," in *Journal of Microelectromechanical Systems*, vol. 31, no. 6, pp. 857-866, Dec. 2022.

[6] P. Ward and A. Duwel, "Oscillator phase noise: systematic construction of an analytical model encompassing nonlinearity," in *IEEE Transactions on Ultrasonics, Ferroelectrics, and Frequency Control*, vol. 58, no. 1, pp. 195-205, January 2011.

CONTACT

*C. Padovani, christian.padovani@polimi.it